Temperature-dependent selectivity for CO electroreduction on copper-based gas-diffusion electrodes at high current densities

Schellekens, M.P.; Raaijman, S.J.; Koper, M.T.M.; Corbett, P.J.

Chemical Engineering Journal 483 (2024) 149105

Contents lists available at ScienceDirect

Chemical Engineering Journal

journal homepage: www.elsevier.com/locate/cej

Temperature-dependent selectivity for CO electroreduction on copper-based gas-diffusion electrodes at high current densities

Maarten P. Schellekens [a,b], Stefan J. Raaijman [b], Marc T. M. Koper [a,*], Paul J. Corbett [b,*]

[a] Leiden Institute of Chemistry, Leiden University PO Box 9502, 2300 RA Leiden, the Netherlands
[b] Energy Transition Campus Amsterdam, Shell Global Solutions International B.V. Grasweg 31, 1031 HW Amsterdam, the Netherlands

ARTICLE INFO

Keywords:
Electrochemistry
CO reduction
Temperature
Conversion

ABSTRACT

The electroreduction of carbon monoxide (CO) on copper (Cu) in aqueous media is known to generate industrially relevant C_{2+} chemicals. CO originating from a CO_2 capture source combined with CO electrolysis, powered with renewable energy and water, provides us with a method of producing green chemicals. However, the industrial applicability of this technology is still in the nascent stage. In this work, we explore the boundaries of what can realistically be achieved with the current state-of-the-art technology, to gauge the feasibility of employing CO reduction as a means of carbon valorization in an industrial setting, focusing on ethylene and ethanol as products of interest due to their market size and value. In this study commercial heterogeneous electrocatalysts were analyzed, applied on a gas diffusion layer (GDL) to form a gas diffusion electrode (GDE) and then ranked with respect to ethylene and ethanol FE. Subsequently, the limits of production rate and single pass conversion were evaluated, and the effect of temperature on product selectivity investigated. Finally, durability under industrially relevant conditions was studied. We found that it is possible to operate at current densities of up to -2500 mA cm^{-2} without any appreciable increase in the faradaic yield towards hydrogen, yielding a total FE to C_{2+} products of 87 % and an ethylene FE of 35 %. We also demonstrate that temperature has a (positive) influence on the FE for ethylene, at the cost of a reduction in acetate formation. Additionally, we show that single pass conversions of up to 89 % can be achieved without loss of FE towards C_{2+} products. However, despite these promising results, we also show that catalyst durability remains a key challenge for long-term industrial operation of CO electroreduction.

1. Introduction

In 2015, the Paris agreement was adopted by 196 parties in the UN Climate Change Conference (COP21), stipulating that global warming from greenhouse gases should not exceed 2 °C above the average global temperature of pre-industrial times. However, in recent years, world leaders have stressed the need to limit global warming to 1.5 °C by the end of this century. To achieve this goal, greenhouse gas emissions must peak before 2025 and decline 43 % by 2030 (relative to the 2019 levels) [1,2].

A straightforward way of reducing net CO_2 emissions without suddenly halting or significantly modifying existing chemical processes is by preventing it from being released into the atmosphere at point sources or alternatively to extract it from the atmosphere after its release via direct air capture. Additional value (beyond reducing emissions) can be derived by taking this CO_2 and converting it into value-added products. With this in mind, we would like to introduce the electroreduction of carbon monoxide (CO) on copper (Cu) in aqueous media, which has the potential to generate a multitude of C_{2+} chemicals that have many industrial uses. CO electrolysis of CO derived from a CO_2 source as just discussed provides us with a method of manufacturing green chemicals. However, industrial applicability of CO electroreduction is still in the nascent stage as it is currently suffering from e.g., poor durability, low single pass conversion and carbon cross-over (of either the reactant(s) and/or products). This is especially true if one is interested in products other than CO and formic acid (HCOOH), such as e.g. ethanol, ethylene, acetaldehyde, acetic acid, and propanol. As these products require more than two electrons to be transferred per CO, the difficulty of optimizing the catalytic pathway imposes additional constraints on the catalyst, which typically results in poorer performance on other (industrially important) areas such as e.g., maximum reaction rates, system stability, product selectivity and maximum achievable

* Corresponding authors.
E-mail addresses: m.koper@lic.leidenuniv.nl (M. T. M. Koper), paul.corbett@shell.com (P.J. Corbett).

https://doi.org/10.1016/j.cej.2024.149105
Received 30 August 2023; Received in revised form 21 November 2023; Accepted 24 January 2024
Available online 1 February 2024

single pass conversion. With ethylene/ethanol having an enormous market size, there exists potential for large-scale reduction of greenhouse gas emissions and commercialisation of such a technology [3–6].

In this work, we explore the boundaries of what can realistically be achieved with the current state-of-the-art technology, to gauge the feasibility of employing CO reduction as a means of carbon valorization in an industrial setting – focusing on ethylene and ethanol as products of interest due to their market size and value. Catalyst selectivity and single pass conversion were studied as strategies to make this technology economically viable, and thus industrially relevant, as they lower post-process separation costs, avoiding one of the most energy-intensive steps [5–7]. Data on the single pass conversion is often missing in scientific literature or, when it is derived from provided mass flow rates, typically conversion levels are low (<50 %).

Here, we focused on the reactant CO rather than CO_2 considering that CO is in a more reduced state than CO_2, meaning that product formation involves the transfer of fewer electrons, which we expected to be beneficial for catalytic performance during the conversion of CO to C_{2+} products [8]. An additional motivation for utilising CO is the acidic nature of CO_2, which limits the alkalinity that can be achieved at the catalyst interface, whilst high alkalinity has been demonstrated to considerably improve catalytic activity towards C_{2+} formation [9,10]. Employing CO instead of CO_2 thus allows for more reproducible interfacial conditions at imposed high pH conditions.

Cu was selected as the catalyst as it has been shown to be capable of achieving acceptable overall performance for producing C_{2+} products in terms of (combined) faraday efficiency (FE) as well as being capable of reaching industrially relevant current densities [11,12]. As such, Cu catalysts were selected from various companies, based on the size of the catalyst particles, variation of companies, and accessibility. In addition, gas diffusion electrodes (GDEs) were employed to bypass the inherent mass transport limitations [13–15] of aqueous (or more generically, solution-phase) electrochemical systems in combination with gaseous reactants. The performance tests of the GDEs were conducted in half cells (H-cells), to investigate the catalytic activity of the cathode in isolation, without running into limitations due to the e.g., membrane or anode performance.

Our experiments show that it is possible to apply cell current densities of up to -2500 mA cm^{-2} without any appreciable increase in the faradaic yield towards hydrogen, with a total FE to C_{2+} of 87 % and an ethylene FE of 35 %. We also demonstrate that temperature has a (positive) influence on the FE for ethylene, whilst the FE to acetate displayed the opposite trend. Finally, we show that single pass conversions of up to 89 % can be achieved without loss of FE towards C_{2+} products at an industrially relevant current density of -1000 mA cm^{-2}. Despite these favorable conversion characteristics, we also show that catalyst durability remains a key challenge for long-term industrial operation of CO electroreduction.

2. Methods

2.1. Chemicals

Electrodes were prepared using a carbon-based gas diffusion layer (GDS2230, Avcarb), Cu nano powder (Sigma-Aldrich, 25 nm), Nafion (520D, 5 wt% in alcohol, FuelCellStore) and isopropanol (Ph Eur, Merck). KOH (99.98 %, Alfa Aesar), H_3PO_4 (85 wt%, GPR rectapur, VWR) and Ultrapure water (Milli-Q gradient, ≥18.2 MΩcm) were used without further purification to prepare the electrolytes. CO (purity 4.7, Linde) and N_2 (purity 4.0, Linde) were used as the reactant and internal standard, respectively.

2.2. GDE preparation

To prepare the various Cu-GDEs, catalyst inks were prepared by sonication (LABSONIC P, Sartorius) of a Cu nano powder and Nafion mixture in isopropanol having concentrations of 4 mg/mL and 7.5 μL /mL, respectively. The GDE was manufactured by spray-painting 0.5 mL/cm^2 of such ink solution onto the carbon-based GDL with an automatic spray-painter (ExactaCoat, Sonotec) with the GDL placed on a heated platform kept at 90 °C. Prior to spray-painting, the GDL was pre-treated via drying in a N_2 purged oven at 90 °C for 30 min. The catalyst layer was deposited via spray-painting layer by layer, with the nozzle being moved from left-to-right whilst additionally being moved up/down in discrete steps, followed by three more passes with the direction of movement being rotated by 90° between subsequent passes, with the nozzle having returned to the starting point by the fourth pass. In-between changing directions, 30 s of rest was afforded for the newly added layer to dry. This four-segment movement was repeated until the ink was consumed. The ink was supplied by a syringe which was sonicated during the 30 s resting periods. In total ca. 90 layers were sprayed, with a total preparation time of 90 min. The electrode sheet was dried overnight under identical conditions to the GDL pre-treatment. The catalyst loading was determined by weighing the dried electrodes, pre- and post-spray, having a typical loading of 0.8 mg/cm^2. The performance of every newly prepared GDE sheet was tested to verify it exhibited catalytic activity comparable to previously obtained results. This was done by determining the FE for H_2 at -1000 mA/cm^2, which was found to typically yield about 7 %, with the GDE being rejected if this value exceeded 10 % (see Fig. S2 for the benchmark results). This verification was conducted to guarantee all experimental conditions were run with a comparable electrode. Higher faradaic efficiencies for HER would sometimes be observed if the ink/tubing was contaminated, or if the spray-painter nozzle was clogged. GDE sheets were stored in closed plastic bags under atmospheric conditions. Electrodes were measured within a period of 2 months of being manufactured.

2.3. Electrochemistry

Reactant gas (CO) was supplied to the cell via a calibrated mass flow controller (Brooks, Delta Smart II). The inlet overpressure of the cell was measured with a manometer (Swagelok) and was typically < 100 mbar.

A glass two compartment H-cell was fabricated in-house, employing a three-electrode configuration (Fig. S1). The working electrode was comprised of a GDE with electrical contact on the backside provided via a stainless-steel current collector containing a serpentine channel via which the CO gas was fed directly to the backside of the GDE. After this the gas is directed into the catholyte compartment. This way of operating renders the pressure difference between the back and the front of the electrode almost negligible, reducing the risk of flooding or gas penetration through the electrode, having a stable boundary layer. A polyether ether ketone (PEEK) mask was placed on top of the GDE to expose a consistent, well-defined area to the electrolyte. The anode was a dimensionally stable anode (Electra-cell) machined in-house to fit the cell geometry. The membrane and anode are roughly 3.5 to 14 times bigger compared to the working electrode depending on the employed mask limiting the cathode area. This reduces the limitations of membrane performance and the challenging OER and allows for only evaluating the performance of the cathode. The backsides of both current collectors were interfaced with a compartment through which temperature-controlled water of typically 25 °C from a thermal bath (Julabo F12) was flowed to control the temperature. For the experiments performed at temperatures other than 25 °C, a double walled electrolysis cell with active flow around the compartments was uses to control the temperature of the full cell, in addition to temperature-controlling the (backsides of the) current collectors. The electrolyte compartments of the H-cell were made of borosilicate glass, with O-rings (made from Viton) being used to ensure leak-tight connections between the various cell components. Individual cell parts were oriented via guiding rods on the outside of the cell and clamped together to assemble the full cell. A reversible hydrogen electrode (GasKatel, Mini HydroFlex) placed in the cathode compartment was used as a reference electrode (RE).

The catholyte (1 M KOH) and anolyte (1 M H_3PO_4) compartments of the cell contained ca. 20 mL of electrolyte and were separated by a cation exchange membrane (FKB-PK-130, Fumatech). The catholyte chamber was agitated in operando using a magnetic stirrer.

An Autolab potentiostat (PGSTAT302N) equipped with an impedance module was operated in galvanostat mode (typically), whilst impedance spectroscopy was ran at operation conditions to determine the solution resistance. Typically, electrode temperature was controlled at 25 °C and a CO inflow of 20 sccm was supplied to the backside of the GDE and then fed into the catholyte compartment. Then, a current density of −50 mA/cm^2 was applied for 2 min, resulting in a total of −6 C/cm^2 applied to the electrode to reduce any copper oxides present at the surface. The catholyte was then replaced to remove any possible liquid products and/or dissolved catalyst. Then, a current density of interest was applied for 30 min. After sampling for liquid analysis and replacing the catholyte, another condition was applied for 30 min. Every individual electrode was used for a maximum of 4 conditions. The total time of 2 h (i.e., 4 runs) was found to be stable for most conditions. Experiments were repeated thrice in most cases to obtain the results reported, though some experiments were performed in duplo. The H-cell was cleaned daily by rinsing thoroughly with Milli-Q water at the start of the first experiment and rinsed in between experiments with fresh electrolyte.

2.4. Analysis

The gas flowing out of the H-cell was mixed with a known N_2 flow, which was used as an internal standard. After, this gas mixture was passed through a dehumidifier (Perma Pure, MD-050-24S-2) to remove water, after which it was directed to the GC (G.A.S, CompactGC 4.0). The GC was equipped with a flame ionization detector (FID) with a Al202/MAPD column and three thermal conductivity detectors (TCD) with two Molsieve 5 A, 60–80 and one Hayesep Q, 60–80 column. Hydrocarbons were analyzed using the FID, other components with the TCDs.

To follow the electrode performance, the gas phase products were analyzed every 5 min. First three datapoints showed stabilization of gas concentrations followed by constant gas concentrations. Only at more extreme conditions the gas concentration for the final datapoints (i.e., >3) changed over time. The data reported for all experiments is an average of the datapoint taken at 30 min for the 2–3 independent runs conducted for a given condition.

The catholyte was sampled after each experiment and analyzed using an off-line High Performance Liquid Chromatography (HPLC) instrument (Agilent Technologies, 1260). The system contained a Hi-Plex H column operated at a temperature of 50 °C. An ultraviolet (UV) and refractive index (RI) detector were used, Injection volume was set to 20 μL and the 10 mM sulfuric acid eluent flow rate was 0.6 mL/min. Acetate was analyzed using the UV detector and ethanol, 1-butanol and allyl alcohol with the RI detector. Typical GC and HPLC chromatograms are given in Figs. S3 and S4, respectively.

3. Results and discussion

3.1. Catalyst selection

An initial screening of commercially available Cu particles was conducted to decide on the type of catalyst to utilize for this study. The various particles were used as received and selectivity optimization through modifying these materials is deemed beyond the scope of the current work. It was purposefully chosen to apply constant-current conditions for this set of experiments, and indeed for the entirety of this study. This was done because we are of the opinion that for GDE systems, constant-current comparison is a fairer metric for comparing cathode performance. Specifically with respect to uncertainties in determining the interfacial potential of GDEs under industrially-relevant operating conditions – which can be split into two aspects. Firstly, the rough and inhomogeneous GDE surface can easily yield a non-uniform potential distribution across it. This results in the potential as determined via a RE situated in the solution phase only representing the region in its vicinity and not necessarily the entirety of the surface. Secondly, because the RE measures the solution-phase potential, it needs to be corrected for ohmic drop to back-calculate the interfacial potential. However, at industrially relevant conditions there is a large flux of gases at any instance (at least in the case of CORR), making resistance measurements conducted under zero-current conditions not representative, and resistance measurements under actual operating conditions to have a high degree of uncertainty. Empirically, we find it is not at all uncommon for resistance measurements to fluctuate on the order of 1 O under semi-high current flows (> |-100 mA/cm2|). As the lower bound for investigated current densities is typically −100 mA/cm2, this would translate to an uncertainty of −100 mV in the interfacial potential as determined by a RE after iR correction. From this perspective, we believe that comparing results on a constant-potential basis would be deceptive; seemingly fair (or even fairer, depending on your perspective) at a first glance, but nonsensical when considering the inaccuracies inherent thereto under the conditions employed herein. A counterargument would be to compare under equal-potential cell voltages as opposed to equal-current conditions, but here a similar reasoning applies: resistance will fluctuate considerably as it now is a function of e.g., the distance and cell geometry, membrane thickness and catalytic activity of both cathode and anode. As such, although we report voltage readings at various instances to align with the customs of the field, we advise the reader to keep in mind the limited meaning of those numbers in this study.

The screening results are displayed in Fig. S5 and detailed in Table S1. These experiments were performed at various current densities (-100, −200 and −300 mA cm^{-2}), with the results at −200 mA cm^{-2} (Fig. S5a) being representative of the overall results. To be comprehensive, the screening results under constant-potential conditions are also shown (ca. −0.85 V vs. RHE, Fig. S5b). TEM images of the various particles are shown in Fig. S6 to S13, showing the morphologies and particles sizes. We opted to employ Cu nanoparticles from Sigma-Aldrich (25 nm) for further studies as they yielded the lowest hydrogen formation at all investigated current densities, one of the highest ethylene FEs and nearly twice the FE for 1-propanol compared to other catalysts. With constant-potential measurements, Sigma-Aldrich (25 nm) particles showed similar trends to constant-current measurements although exhibiting a significantly higher current density of −1000 mA cm^{-2} (vs. −200–300 mA cm^{-2} for the other catalyst investigated at this potential). Cu nanoparticles from Sigma-Aldrich (25 nm) and most of the other screened Cu catalysts exhibited a similar CORR product distribution when hydrogen is excluded, in line with the product distribution of pure Cu based catalyst reported elsewhere. Although the selectivity is suboptimal from an industrial perspective, copper is the current best CORR catalyst with respect to C_{2+} product formation. We'd like to reiterate that the aim of this study is to investigate what can realistically be achieved with the current state-of-the-art technology, to gauge the feasibility of employing CO reduction as a means of carbon valorization in an industrial setting and not to identify/create a novel material with superior performance, nor to ascertain why any material performs better than another.

3.2. Catalyst characterization

Using the Sigma-Aldrich (25 nm) Cu catalyst, we performed some internal optimizations of GDE formulations such as which substrate to use, coating thickness and ink composition – though this was rather rudimentary and therefore will not be discussed in detail herein (except for the pertinent information provided in the experimental section). Our TEM analysis (Fig. 1 a-b) shows the catalyst has an open structure consisting of individual strands of ca. 50–100 nm that clustered together

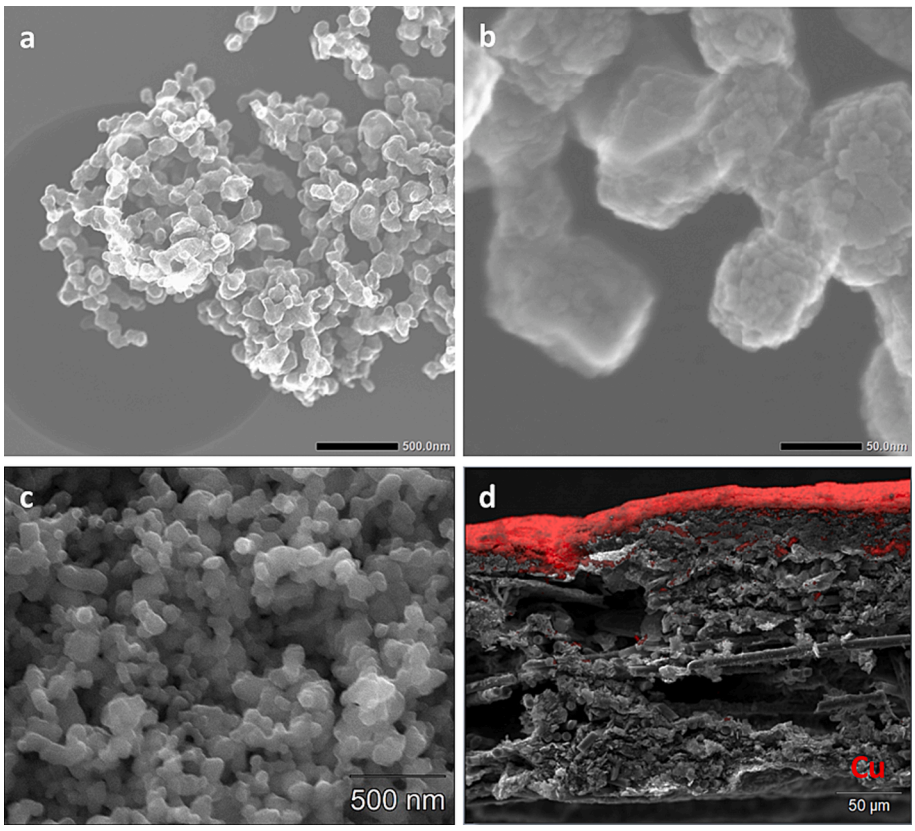

Fig. 1. (a,b) TEM image of Sigma Aldrich (25 nm) catalyst separately, (c) SEM image from topside of Sigma Aldrich (25 nm) coated on GDL, (d) SEM-EDS Cross-section of this GDE.

to form a porous network, like a micro foam. By subsequently stacking this foam-like material during the spray-painting process, we obtain a catalyst layer that remains porous and highly permeable to gas (Fig. 1c). This likely results in effective mass transport between the gas-facing and electrolyte-facing sides of the catalyst layer, resulting in the generation of the highly important triple junction where catalyst, gaseous reactant and liquid electrolyte come together, without the water layer penetrating too deeply into the catalyst layer and thereby forcing gas to diffuse through a liquid layer/film [16]. A cross-section of the GDE, superimposed with EDX results (Fig. 1d) gives the location of Cu present within the GDE; from this, it can be estimated that the catalyst layer has a thickness between 25 and 50 µm.

Subsequently, we assessed several industrially relevant system parameters on the semi-optimized GDE. The purpose of this endeavor was to explore the upper boundaries of the system in terms of current density, attainable reactant conversion and electrode durability during the

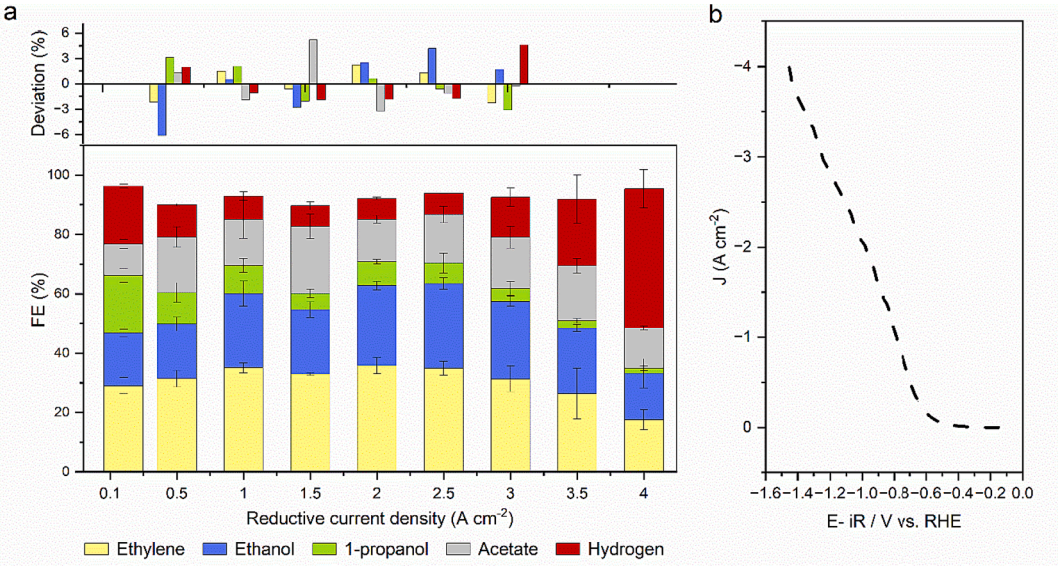

Fig. 2. A) Product distribution for stepped-current experiments employing 1 M KOH catholyte, at a controlled temperature of 25 °C and a reactant flowrate of 20 sccm with product deviation given between −0.5 and −3 A cm^{-2} and **b)** total geometric current density vs. potential.

CORR to ascertain the industry-readiness level of this technology.

3.3. Current density boundaries and effects

The first parameter of interest was current density, to investigate what the apparent limits of appropriately combined commercially available components are. As displayed in Fig. 2a, industrially relevant current densities can be achieved on the optimized GDE employed throughout this work [4,5]. The electrode stability as measured by GC and potential over time is depicted in Fig. S14, showing relatively stable performance for current densities up to and including −2000 mA/cm^2, but for higher current densities strong fluctuations in potential are observed and HER is starting to dominate. Interestingly, a FE of < 10 % to hydrogen was observed to be feasible up to a current density of −2500 mA cm^{-2} (with even −3000 mA cm^{-2} yielding a respectably low hydrogen FE of ca. 15 %), meaning that most of the current is being used for the intended purpose, i.e., carbon valorization. These experiments were performed with an excess of CO feed meaning low conversion.

For our experiments, we typically observe total faradaic efficiency values slightly below 100 %. Contrary to missing minority products or measurement error, we believe this can be explained by the following considerations. Firstly, partial evaporation of alcoholic components results in a slight underestimation of the FE for such components. Secondly, there is always some amount of product crossover that occurs during electrochemical experiments, meaning some products are lost to the anode where they may either be oxidized into CO_2 or partially oxidized into products other than the actual CO2RR product spectrum. As such, a slightly lower total FE than 100 % is quite common in the CORR and CO2RR studies [17,18].

A remarkable observation for this optimized GDE that has significant industrial relevance, is that there exists a broad range where increasing the current density (and thus increasing the (cell) potential) has limited impact on the product distribution. This regime is captured in Fig. 2a, wherein we plot the deviation from the mean for the observed products between −500 and −3000 mA cm^{-2}, showing that the deviation is never more than 6 %. This behavior is expected to be beneficial from an intermittency perspective, as the current can be increased or decreased according to local electricity availability whilst the product composition remains largely unaffected (presuming that the reactant inflow is scaled proportionally to the current). This behavior, however, is quite unlike most reported literature, as generally an optimum is observed for ethylene formation as a function of potential on Cu-catalyzed systems. Although such an optimum in potential is more commonly observed for CO2RR systems [19] as opposed to CORR systems, it has also been observed for the latter [8,20–22]. The apparent conflict in observed behavior can readily be addressed by considering that our operating current window is significantly higher than most CORR studies, especially when combined with the observation that the observed onset of this deviant behavior is at current densities more than −500 mA cm^{-2}.

An additional (possible) explanation for why previous observations have shown a potential dependency of the product distribution whereas our experiments show only little, would be as a result from (differences in) heat management. Active temperature control is quite uncommon for a H-cell. As part of our optimization strategy, we have also investigated the effect of temperature and found that, at elevated temperatures, ethylene becomes more favorable, as will be discussed in the next section.

3.4. Temperature boundaries and effects

Temperature-controlled experiments were performed in a double-walled glass H-cell, with the backside of the GDE and the outer compartment of the cell being heated (or cooled) via a constant flow of temperature-controlled water. Experiments were performed at low conversion and a constant current of −500 mA cm^{-2}. The effect of temperature on the product distribution is depicted in Fig. 3. From 5 °C

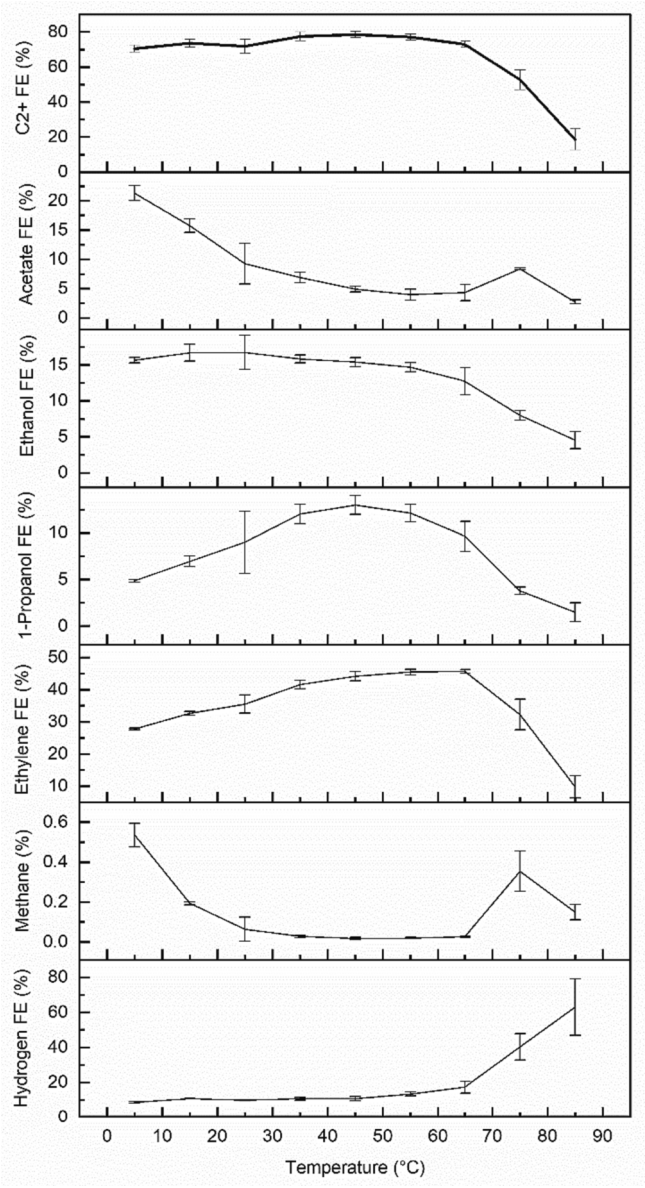

Fig. 3. CORR product selectivity plotted as a function of cell temperature. Performed at a constant current of 500 mA/cm^2 and 20 SCCM CO.

to 65 °C, there is an absolute increase in the faradaic efficiency for ethylene from 29 % to 47 %, before dropping rapidly when the temperature is increased further. For 1-propanol a similar effect is observed, although the optimum FE is observed to be earlier; around 45 °C. Ethanol and hydrogen formation are less influenced by temperature with the former showing a constant but mild decay in FE and the latter the opposite in the form of a mild increase. However, at temperatures higher than 65 °C, hydrogen formation was observed to increase rapidly. Importantly, acetate formation is strongly inhibited by increasing the temperature, dropping from ca. 21 % FE (at 5 °C) to less than 5 % at the highest temperature investigated (85 °C).

These results clearly show the sensitivity of CORR product distribution in relation with temperature and, thereby, the relevance of controlling the temperature accurately during electrochemical CORR experiments. We expect this conclusion to extend to CO2RR experiments, especially when higher current densities are employed. This could also explain some of the selectivity differences seen by other authors [20,21] reporting improved FE towards ethylene at higher current densities, where the generated heat starts to become more difficult to

dissipate.

Although the observed trend is in favor of industrial applicability, above 65 °C the HER rapidly overtakes the CORR. As for why hydrogen evolution starts to outcompete CORR, we can only speculate at this moment in time. We hypothesize that this may be related to a change in GDL hydrophobicity, resulting in flooding of the GDE or possibly it could be a reconfiguration of the catalyst particles on the atomic scale due to an increased atom mobility at elevated temperatures. With the shift towards HER resulting in much larger volumes of gas evolved around the GDL/catalyst/ionomer layer, it might be that the morphology of the complex GDE is changed, like delamination of the ionomer layer from the Cu particles. Our testing in this area was not in detail for this study, the only relevant information that we can provide is that HER activity remains at elevated levels compared to an original GDE, if the electrode is firstly subjected to operation at 85 °C prior to conducting experiments at milder temperatures (Fig. S15). On Copper and gold foil electrodes, there is a seemingly similar temperature-dependent competition between the HER and (in their case) CO2RR starting from ca. 55 °C during rotating ring disk experiments in aqueous solutions [23,24].

From an industrial perspective, the observed trend where ethylene selectivity is improved at elevated temperatures (mostly at the cost of acetate and ethanol formation) is highly beneficial due to the significant costs associated with downstream product separation. In addition, electrolyte resistances are decreased at elevated temperatures which in turn yield a lower electrode (see Fig. S16) and overall cell potential, translating to an improved energy efficiency. This becomes even more apparent when one considers that ohmic losses lead to in-situ heat generation, meaning that operation at lower temperatures whilst applying equivalent current densities would incur further energy penalties in the form of cooling as required to remove the additionally generated heat. Besides this, an increase in temperature also has the effect of increasing the vapor pressure of liquid products such as ethanol and propanol, which are formed as by-products. Increasing the vapor pressure would decrease the likelihood of condensation of such products into droplets, which would in turn be beneficial in preventing product-induced flooding and thus system stability. Finally, operation at elevated temperatures allows for easier integration with other industrial processes such as CO generated through the reverse water–gas shift reaction or downstream product separation through distillation.

3.5. Single-pass conversion

We continued by investigating the effect of reactant flow rate and, by association, the single pass conversion on the catalytic performance of our optimized GDE. Results are given in Fig. 4. The product selectivity (Fig. 4 a-b) is relatively stable over the whole range of tested flowrates, however the HER becomes more prominent at the lower flowrates. At the lowest flowrates tested at −500 and −1000 mA cm ^{2} the observed single pass conversions were highest at 92.7 and 92.5 %, respectively. The measured composition of the gaseous product stream coming out of the H-cell is given in Fig. 4 c-d, where lower inlet flows coupled with equivalent total applied currents yield increased CO consumption, resulting in a lower partial pressure for CO. With the highest conversions only 12.2 and 11.3 v% CO is remaining at the end of the cell for −500 and −1000 mA cm^{-2}, respectively.

Traditionally, product faradaic efficiencies are used to represent results in electrochemically oriented publications, which yields favorable results in our situation with respect to the relatively minor amount of current going to make hydrogen. However, when looking at the actual gas composition (in vol%) the amount of hydrogen is typically similar to- or even higher than ethylene, making post-reaction separation energy intensive. Hence, even though we achieve single pass conversions of up to 89 % of CO at an industrially relevant current density of −1000 mA cm^{-2}, the resulting product stream (containing ca. 38 vol% of ethylene, 40 vol% hydrogen and 21 vol% CO) is not quite as good as the more common metric (FE) would have one believe [21,25–27].

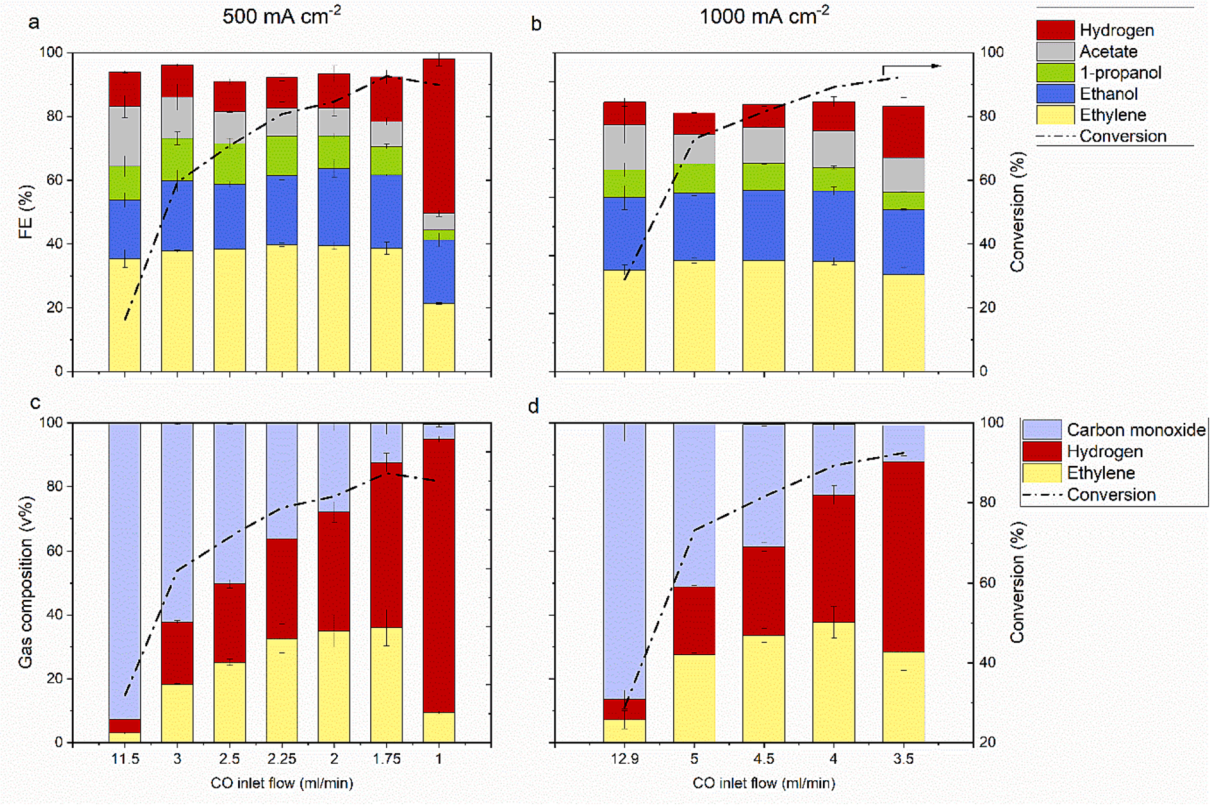

Fig. 4. Conversion as a result of CO inlet flow to the electrolchemical cll, plotted as a function of CORR products (FE) at (a) −500 mA cm^{-2} and (b) −1000 mA cm^{-2} and plotted against the final gas compasition from the electrochemical cell at (c) −500 mA cm^{-2} and (d) −1000 mA cm^{-2}.

Beside the apparent benefits for industrial application, the observation that the FE is almost unchanged when the partial CO pressure is decreased by a factor of ca. 4.5 (going to from 100 vol% to 22 vol%) is intriguing, though understanding why deserves more attention than the current scope of this work allows for. In other systems where the $CO_{(2)}$ partial pressure has been investigated, such a decrease in partial pressure typically influences the carbon-derived product spectrum significantly, and hydrogen formation typically becoming more prominent as partial pressure is decreased.[10,28]. At this moment in time, the origin of this behavior eludes us though we believe it to be highly relevant for industrial application and intend to investigate in more detail. Although without concrete proof, we feel the high surface area combined with the morphology of the catalyst layer play an integral role in allowing for the creation of the triple phase boundary that is necessary for achieving high current densities reported herein (i.e., up to -3 A/cm^2). We feel this line of reasoning is partially substantiated by the high conversion rates we obtained, which strongly hint at sufficiently rapid gas exchange at the interface such that reactant starvation seems not to be taking place to a significant degree (as the combined FE for the CORR was still in excess of 80 %).

3.6. Durability

Finally, we investigated electrode durability, although we would like to preface this discussion with the notion that durability tests conducted on a small area GDE in an H-cell environment as used throughout this work will not be directly comparable with durability in an industrial optimized electrolyser environment. For economically viable operation of an electrolyser, system durability requires operation in the order of thousands of hours, like water electrolysers as an example are stable for about 20,000 h[6].

Fig. 5 shows that ethylene formation is relatively stable over ca. 5, 10 and 50 h at current densities of -1000, -500 and -200 mA cm^{-2}, respectively. After this window, Hydrogen formation is rapidly taking over from CORR meaning deactivation of the electrode. Although, for the formation of one CORR product methane, it was observed that it follows a similar trend as hydrogen formation, suggesting that methane formation is an indication of deactivation. As expected, durability is increased with decreasing current densities, but if the FE is plotted against the number of coulombs instead of time (Fig. S17) the durability of these three tested current densities gets more comparable. However, the lowest current density tested still shows a longer stability for ethylene formation. Durability's in this order of magnitude are often observed in literature for reduction with Cu based systems [21,29–31].

It must be noted that the wide array of products that are formed during the reaction (Fig. 2a) is likely to have a significant impact on durability and industrial applicability. The latter is self-explanatory; making products that are not your intended target results in increased separation costs, and these parasitic products typically have a lower market value and/or trading volume. However, the durability implications of such a diverse product distribution may well prove more detrimental for industrial applicability, especially the large quantity of alcoholic species. Not only will these alcohols deteriorate the membranes that are necessary to isolate the products formed at the cathode from the oxidants formed at the anode (i.e., a stringent safety consideration), but their accumulation will also influence the catalyst via significantly changing the local environment. In addition, a GDE relies significantly on hydrophobic components (typically PTFE) to prevent aqueous components from penetrating and irreversibly filling the pores where the tri-phase boundary region exists. However, this hydrophobic protection is substantially reduced for alcohol/water mixtures [32], resulting in expedited flooding which in turn hampers industrial application.

4. Conclusions

In this work we screened multiple commercial catalysts for their electrochemical CORR performance and found that the 25 nm Cu

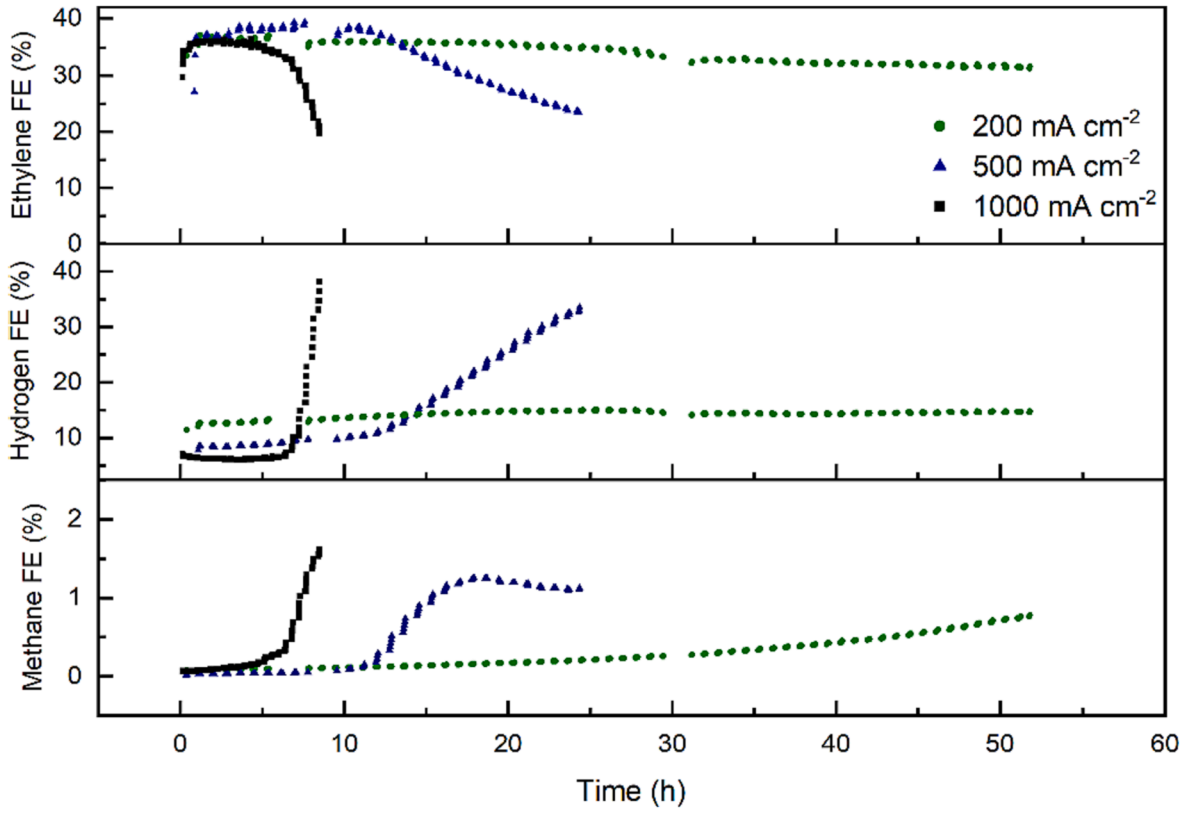

Fig. 5. Durability test at constant currents -200, -500 and -1000 mA cm^{-2}, 1 M KOH, 20 SCCM and 25 °C.

nanoparticles from Sigma Aldrich had the lowest FE for HER and additionally required the lowest overpotential for yielding a given current. After some optimization steps post-catalyst selection, we explored the boundaries of what can realistically be achieved in terms of industrially relevant CORR performance metrics (current density, selectivity, conversion, and durability).

We were able to drive the cell at current densities of up to −2500 mA cm^{-2} without any appreciable increase in the faradaic yield towards hydrogen, with a total FE to C_{2+} of 87 % (35 % ethylene, 29 % ethanol, 16 % acetate, 7 % 1-propanol). Between −500 and −3000 mA cm^{-2}, a largely static product distribution was observed, something we believe is related to a combination of the higher current densities we apply and the efficient mass transport of gaseous species through the GDE to the solution-facing side of the catalyst layer. Furthermore, because of the design of the cell we can negate temperature effects which, we found, had a large influence on the selectivity of CORR-related products with the FE for ethylene increasing with temperature, and the FE to acetate showing the opposite trend.

We also demonstrated that single pass conversions of 89 % could be achieved without increasing hydrogen formation substantially at an industrially relevant current density of −1000 mA cm^{-2} and we could even push the system to 92 % conversion if an absolute increase in the HER FE of 7.7 % would be considered acceptable (which depends mostly on the cost-balance between removing unconverted reactant vs. removing additional hydrogen and a decrease in efficient electron utilization).

Finally, we touch upon the electrode durability, which we find is poor with regards to industrial standards and is negatively correlated to the applied current density. Deactivation appears to be accompanied with enhanced methane formation, suggesting graphite formation as a possible cause.

CRediT authorship contribution statement

Maarten P. Schellekens: Conceptualization, Data curation, Formal analysis, Investigation, Methodology, Validation, Writing – original draft. **Stefan J. Raaijman:** Conceptualization, Data curation, Formal analysis, Investigation, Writing – original draft, Writing – review & editing. **Marc T. M. Koper:** Conceptualization, Validation, Writing – review & editing, Supervision. **Paul J. Corbett:** Conceptualization, Formal analysis, Funding acquisition, Project administration, Resources, Supervision, Validation, Visualization, Writing – review & editing.

Declaration of competing interest

The authors declare that they have no known competing financial interests or personal relationships that could have appeared to influence the work reported in this paper.

Data availability

Data will be made available on request.

Appendix A. Supplementary data

Supplementary data to this article can be found online at https://doi.org/10.1016/j.cej.2024.149105.

References

[1] M. Meinshausen, N. Meinshausen, W. Hare, S.C. Raper, K. Frieler, R. Knutti, D. J. Frame, M.R. Allen, Greenhouse-gas emission targets for limiting global warming to 2 degrees C, Nature 458 (2009) 1158–1162, https://doi.org/10.1038/nature08017.

[2] C. McGlade, P. Ekins, The geographical distribution of fossil fuels unused when limiting global warming to 2 degrees C, Nature 517 (2015) 187–190, https://doi.org/10.1038/nature14016.

[3] M. Jouny, G.S. Hutchings, F. Jiao, Carbon monoxide electroreduction as an emerging platform for carbon utilization, Nature Catalysis 2 (2019) 1062–1070, https://doi.org/10.1038/s41929-019-0388-2.

[4] J. Sisler, S. Khan, A.H. Ip, M.W. Schreiber, S.A. Jaffer, E.R. Bobicki, C.-T. Dinh, E. H. Sargent, Ethylene electrosynthesis: a comparative techno-economic analysis of alkaline vs membrane electrode assembly vs CO2–CO–C2H4 tandems, ACS Energy Lett. 6 (2021) 997–1002, https://doi.org/10.1021/acsenergylett.0c02633.

[5] M.G. Kibria, J.P. Edwards, C.M. Gabardo, C.T. Dinh, A. Seifitokaldani, D. Sinton, E. H. Sargent, Electrochemical CO2 reduction into chemical feedstocks: from mechanistic electrocatalysis models to system design, Adv Mater 31 (2019) e1807166.

[6] M. Jouny, W. Luc, F. Jiao, General techno-economic analysis of CO2 electrolysis systems, Ind. Eng. Chem. Res. 57 (2018) 2165–2177, https://doi.org/10.1021/acs.iecr.7b03514.

[7] T. Alerte, J.P. Edwards, C.M. Gabardo, C.P. O'Brien, A. Gaona, J. Wicks, A. Obradović, A. Sarkar, S.A. Jaffer, H.L. MacLean, D. Sinton, E.H. Sargent, Downstream of the CO2 electrolyzer: assessing the energy intensity of product separation, ACS Energy Lett. 6 (2021) 4405–4412, https://doi.org/10.1021/acsenergylett.1c02263.

[8] N.S. Romero Cuellar, K. Wiesner-Fleischer, M. Fleischer, A. Rucki, O. Hinrichsen, Advantages of CO over CO2 as reactant for electrochemical reduction to ethylene, ethanol and n-propanol on gas diffusion electrodes at high current densities, Electrochimica Acta 307 (2019) 164–175, https://doi.org/10.1016/j.electacta.2019.03.142.

[9] X. Liu, P. Schlexer, J. Xiao, Y. Ji, L. Wang, R.B. Sandberg, M. Tang, K.S. Brown, H. Peng, S. Ringe, C. Hahn, T.F. Jaramillo, J.K. Norskov, K. Chan, pH effects on the electrochemical reduction of CO(2) towards C2 products on stepped copper, Nat Commun 10 (2019) 32, https://doi.org/10.1038/s41467-018-07970-9.

[10] L. Wang, S.A. Nitopi, E. Bertheussen, M. Orazov, C.G. Morales-Guio, X. Liu, D. C. Higgins, K. Chan, J.K. Nørskov, C. Hahn, T.F. Jaramillo, Electrochemical carbon monoxide reduction on polycrystalline copper: effects of potential, pressure, and ph on selectivity toward multicarbon and oxygenated products, ACS Catal. 8 (2018) 7445–7454, https://doi.org/10.1021/acscatal.8b01200.

[11] Y. Hori, Electrochemical CO2 Reduction on Metal Electrodes, in: C.G. Vayenas, R. E. White, M.E. Gamboa-Aldeco (Eds.), Modern Aspects of Electrochemistry, Springer New York, New York, NY, 2008, pp. 89–189.

[12] S. Nitopi, E. Bertheussen, S.B. Scott, X. Liu, A.K. Engstfeld, S. Horch, B. Seger, I.E. L. Stephens, K. Chan, C. Hahn, J.K. Norskov, T.F. Jaramillo, I. Chorkendorff, Progress and perspectives of electrochemical CO2 reduction on copper in aqueous electrolyte, Chem Rev 119 (2019) 7610–7672, https://doi.org/10.1021/acs.chemrev.8b00705.

[13] H. Rabiee, L. Ge, X. Zhang, S. Hu, M. Li, Z. Yuan, Gas diffusion electrodes (GDEs) for electrochemical reduction of carbon dioxide, carbon monoxide, and dinitrogen to value-added products: a review, Energ. Environ. Sci. 14 (2021) 1959–2008, https://doi.org/10.1039/d0ee03756g.

[14] Y. Luo, K. Zhang, Y. Li, Y. Wang, Valorizing carbon dioxide via electrochemical reduction on gas-diffusion electrodes, InfoMat 3 (2021) 1313–1332, https://doi.org/10.1002/inf2.12253.

[15] X. Li, C. Peng, J.P. Crawshaw, G.C. Maitland, J.P.M. Trusler, The pH of CO2-saturated aqueous NaCl and NaHCO3 solutions at temperatures between 308 K and 373 K at pressures up to 15 MPa, Fluid Phase Equilib. 458 (2018) 253–263, https://doi.org/10.1016/j.fluid.2017.11.023.

[16] T. Moore, X. Xia, S.E. Baker, E.B. Duoss, V.A. Beck, Elucidating mass transport regimes in gas diffusion electrodes for CO2 electroreduction, ACS Energy Lett. 6 (2021) 3600–3606, https://doi.org/10.1021/acsenergylett.1c01513.

[17] K.P. Kuhl, E.R. Cave, D.N. Abram, T.F. Jaramillo, New insights into the electrochemical reduction of carbon dioxide on metallic copper surfaces, Energ. Environ. Sci. 5 (2012) 7050, https://doi.org/10.1039/c2ee21234j.

[18] J.E. Pander Iii, D. Ren, B.S. Yeo, Practices for the collection and reporting of electrocatalytic performance and mechanistic information for the CO2reduction reaction, Catalysis Sci. Technol. 7 (2017) 5820–5832, https://doi.org/10.1039/c7cy01785e.

[19] Y. Hori, A. Murata, R. Takahashi, Formation of hydrocarbons in the electrochemical reduction of carbon dioxide at a copper electrode in aqueous solution, J. Chem. Soc., Faraday Trans. 1 85 (1989) 2309–2326, https://doi.org/10.1039/F19898502309.

[20] J. Li, K. Chang, H. Zhang, M. He, W.A. Goddard, J.G. Chen, M.-J. Cheng, Q. Lu, Effectively increased efficiency for electroreduction of carbon monoxide using supported polycrystalline copper powder electrocatalysts, ACS Catal. 9 (2019) 4709–4718, https://doi.org/10.1021/acscatal.9b00099.

[21] D.S. Ripatti, T.R. Veltman, M.W. Kanan, Carbon monoxide gas diffusion electrolysis that produces concentrated C2 products with high single-pass conversion, Joule 3 (2019) 240–256, https://doi.org/10.1016/j.joule.2018.10.007.

[22] X. Fu, J. Zhang, Y. Kang, Electrochemical reduction of CO2 towards multi-carbon products via a two-step process, React. Chem. Eng. 6 (2021) 612–628, https://doi.org/10.1039/d1re00001b.

[23] R.E. Vos, M.T.M. Koper, The effect of temperature on the cation-promoted electrochemical CO2 reduction on gold, ChemElectroChem 9 (2022), https://doi.org/10.1002/celc.202200239.

[24] R.E. Vos, K.E. Kolmeijer, T.S. Jacobs, W. van der Stam, B.M. Weckhuysen, M.T. M. Koper, How temperature affects the selectivity of the electrochemical CO(2) reduction on copper, ACS Catal 13 (2023) 8080–8091, https://doi.org/10.1021/acscatal.3c00706.

[25] H.P. Duong, N.-H. Tran, G. Rousse, S. Zanna, M.W. Schreiber, M. Fontecave, Highly selective copper-based catalysts for electrochemical conversion of carbon

monoxide to ethylene using a gas-fed flow electrolyzer, ACS Catal. 12 (2022) 10285–10293, https://doi.org/10.1021/acscatal.2c03143.
[26] C.P. O'Brien, R.K. Miao, S. Liu, Y. Xu, G. Lee, A. Robb, J.E. Huang, K. Xie, K. Bertens, C.M. Gabardo, J.P. Edwards, C.-T. Dinh, E.H. Sargent, D. Sinton, Single pass CO2 conversion exceeding 85% in the electrosynthesis of multicarbon products via local CO2 regeneration, ACS Energy Lett. (2021) 2952–2959, https://doi.org/10.1021/acsenergylett.1c01122.
[27] A. Ozden, J. Li, S. Kandambeth, X.-Y. Li, S. Liu, O. Shekhah, P. Ou, Y. Zou Finfrock, Y.-K. Wang, T. Alkayyali, F. Pelayo García de Arquer, V.S. Kale, P.M. Bhatt, A.H. Ip, M. Eddaoudi, E.H. Sargent, D. Sinton, Energy- and carbon-efficient CO2/CO electrolysis to multicarbon products via asymmetric ion migration–adsorption, Nature Energy, (2023). 10.1038/s41560-022-01188-2.
[28] M. Moradzaman, C.S. Martínez, G. Mul, Effect of partial pressure on product selectivity in Cu-catalyzed electrochemical reduction of CO2, Sustainable Energy Fuel 4 (2020) 5195–5202, https://doi.org/10.1039/d0se00865f.
[29] M. Zhong, K. Tran, Y. Min, C. Wang, Z. Wang, C.T. Dinh, P. De Luna, Z. Yu, A. S. Rasouli, P. Brodersen, S. Sun, O. Voznyy, C.S. Tan, M. Askerka, F. Che, M. Liu, A. Seifitokaldani, Y. Pang, S.C. Lo, A. Ip, Z. Ulissi, E.H. Sargent, Accelerated discovery of CO2 electrocatalysts using active machine learning, Nature 581 (2020) 178–183, https://doi.org/10.1038/s41586-020-2242-8.
[30] R.K. Miao, Y. Xu, A. Ozden, A. Robb, C.P. O'Brien, C.M. Gabardo, G. Lee, J. P. Edwards, J.E. Huang, M. Fan, X. Wang, S. Liu, Y. Yan, E.H. Sargent, D. Sinton, Electroosmotic flow steers neutral products and enables concentrated ethanol electroproduction from CO2, Joule 5 (2021) 2742–2753, https://doi.org/10.1016/j.joule.2021.08.013.
[31] C.-T. Dinh, T. Burdyny, M.G. Kibria, A. Seifitokaldani, C.M. Gabardo, F.P. García de Arquer, A. Kiani, J.P. Edwards, P. De Luna, O.S. Bushuyev, C. Zou, R. Quintero-Bermudez, Y. Pang, D. Sinton, E.H. Sargent, CO2 electroreduction to ethylene via hydroxide-mediated copper catalysis at an abrupt interface, Science 360 (2018) 783–787, https://doi.org/10.1126/science.aas9100.
[32] B. Sahin, S. Kimberly Raymond, F. Ntourmas, R. Pastusiak, K. Wiesner-Fleischer, M. Fleischer, E. Simon, O. Hinrichsen, Accumulation of liquid byproducts in an electrolyte as a critical factor that compromises long-term functionality of CO(2)-to-C(2)H(4) electrolysis, ACS Appl Mater Interfaces 15 (2023) 45844–45854, https://doi.org/10.1021/acsami.3c08454.